Marine Chemistry 243 (2022) 104135

Contents lists available at ScienceDirect

Marine Chemistry

journal homepage: www.elsevier.com/locate/marchem

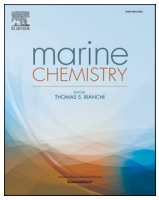

Isotopic evolution of dissolved Ni, Cu, and Zn along the Kuroshio through the East China Sea

Shotaro Takano [a,*], Wen-Hsuan Liao [b], Tung-Yuan Ho [c], Yoshiki Sohrin [a]

[a] Institute for Chemical Research, Kyoto University, Kyoto, Japan
[b] CNRS, University of Brest, IRD, Ifremer, LEMAR, Plouzané, France
[c] Research Center for Environmental Changes, Academia Sinica, Taipei, Taiwan

ARTICLE INFO

Keywords:
GEOTRACES
Coastal region
Source apportionment
Trace metals
Nontraditional stable isotopes

ABSTRACT

In this study, we have investigated the evolution of concentrations and isotope ratios of dissolved nickel (Ni), copper (Cu), and zinc (Zn) from the North Equatorial Current in the western North Pacific to the Kuroshio in the East China Sea, where the inputs of anthropogenic and lithogenic materials through riverine and aeolian pathways are relatively high. The concentrations and isotope ratios for Ni, Cu, and Zn in the deep water of the East China Sea are similar to those of the western North Pacific. The concentrations of Ni, Cu, and Zn in the Changjiang diluted water (<34.0 of salinity) are 3.0–4.1 nmol/kg, 2.0–2.7 nmol/kg, and 0.5–1.1 nmol/kg, respectively, which are significantly higher than those in the surface water of the western North Pacific, thereby indicating the impact of the riverine input. In the Changjiang diluted water, isotope ratios of Ni range from +0.8 to +1.4‰, which is lower than +1.7‰ observed in the surface water (<150 m) of the western North Pacific. The distribution of concentrations and isotope ratios for dissolved Ni fit with simple mixing among the three end-members, Changjiang diluted water, Kuroshio surface water, and deep water in the western North Pacific. A mixing model using isotope ratios and concentrations for Ni quantitatively evaluates the sources of dissolved Ni in the East China Sea. The ranges of the isotope ratios are +0.4 to +0.5‰ for Cu and −0.1 to +0.2‰ for Zn in the Changjiang diluted water, which are similar to those in the surface water of the Okinawa Trough but lower than those in the distal ocean, such as the central Pacific. Compared with published data from the global ocean, dissolved Ni, Cu, and Zn are isotopically lighter in the surface water of some coastal regions than in the pelagic regions, indicating that isotopically light Ni, Cu, and Zn are supplied from the continents.

1. Introduction

Trace metals, including nickel (Ni), copper (Cu), and zinc (Zn), are micronutrients or toxins for marine phytoplankton; their distribution and biogeochemical cycling information are essential for understanding the phytoplankton community structure and material cycling in the ocean (Brand et al., 1986; Morel and Price, 2003). Their biogeochemical cycles can influence the carbon cycle and, ultimately, the global climate. Currently, global distributions of the concentrations and isotopic ratios for Ni, Cu, and Zn in the ocean are mainly revealed by the GEOTRACES program (Schlitzer et al., 2018). These distributions have provided important information on the sources and sinks of Ni, Cu, and Zn, as well as their behavior in the interior ocean. In terms of Ni, the concentrations range from 2 to 6 nmol/kg in the surface water (<50 m) and increase with depth in the ocean (e.g., Middag et al., 2020; Vu and Sohrin, 2013; Wang et al., 2019), reaching a maximum of 10 nmol/kg at 1000–3000 m in the North Pacific (Zheng et al., 2021). The isotope ratios of Ni (δ^{60}Ni) are higher in the surface water than those in deeper water, with a maximum of +1.8‰ observed in the oligotrophic South Pacific (Takano et al., 2017), and becomes nearly uniform at +1.3‰ at depths greater than 1000 m (Archer et al., 2020; Cameron and Vance, 2014; Takano et al., 2017; Wang et al., 2019; Yang et al., 2020; Yang et al., 2021). Such isotopic distribution for Ni is explained by the preferential biological uptake of lighter isotopes in the surface water and remineralization of biogenic particles in deeper water.

Zinc concentrations are 0–2 nmol/kg in the surface water (< 50 m) and increase with depth (e.g., Conway and John, 2014; Croot et al., 2011; John et al., 2018; Middag et al., 2019; Samanta et al., 2017; Vu and Sohrin, 2013; Wang et al., 2019), reaching a maximum of 10 nmol/kg at 1000–3000 m in the North Pacific (Conway and John, 2015; Vance

* Corresponding author.
E-mail address: takano.shotaro.3r@kyoto-u.ac.jp (S. Takano).

https://doi.org/10.1016/j.marchem.2022.104135
Received 25 January 2022; Received in revised form 27 April 2022; Accepted 22 May 2022
Available online 28 May 2022

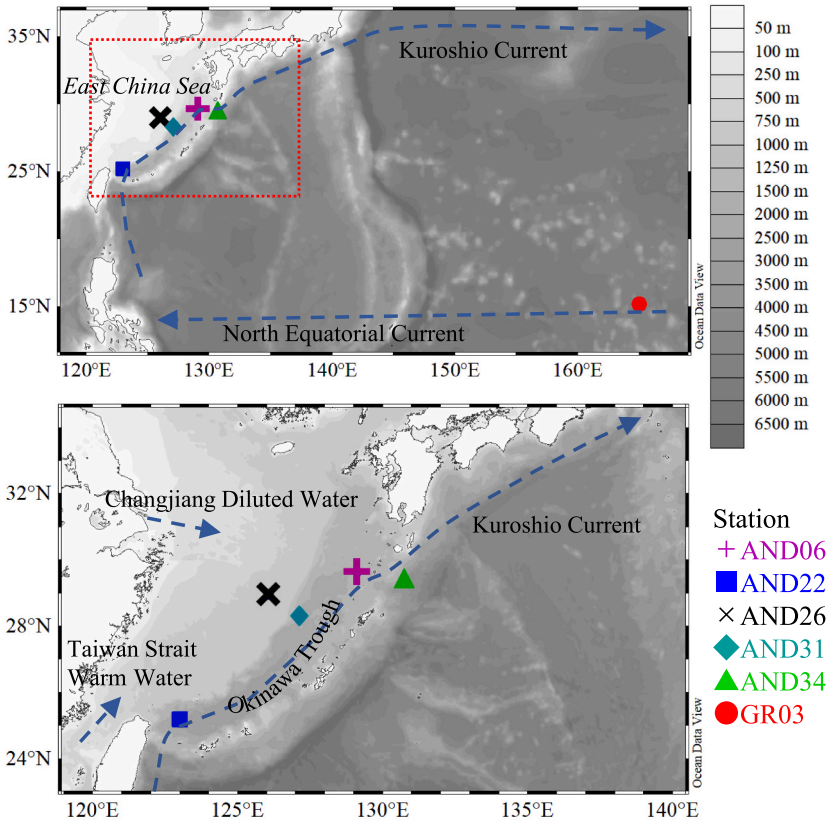

Fig. 1. Sampling sites. The upper panel shows the sampling sites and the flow paths of the North Equatorial Current and the Kuroshio Current. The lower panel shows an enlarged map indicated by the red square in the upper panel. The inflow of the Changjiang Diluted Water and Taiwan Strait Warm Water are also shown. (For interpretation of the references to colour in this figure legend, the reader is referred to the web version of this article.)

et al., 2019; Zheng et al., 2021). Isotope ratios of Zn (δ^{66}Zn) vary from −0.8 to +0.8‰ in the surface water and are constant at ~0.5‰ in the deep water (>1000 m) (Conway and John, 2014; Conway and John, 2015; John et al., 2018; Lemaitre et al., 2020; Liao, 2020; Samanta et al., 2017;Vance et al., 2019; Zhao et al., 2014). Previous studies have shown that the processes controlling the isotopic distribution of Zn in the ocean include the uptake of isotopically light Zn by phytoplankton (John and Conway, 2014; Köbberich and Vance, 2019), adsorption of isotopically heavy Zn on particles (John and Conway, 2014), and the supply of isotopically light Zn from atmospheric and sedimentary sources (Lemaitre et al., 2020; Liao et al., 2020).

Copper concentrations range from 0.5 to 2 nmol/kg in the surface water (< 50 m),(e.g., Boye et al., 2012; Roshan and Wu, 2015; Ruacho et al., 2020; Vu and Sohrin, 2013) and gradually increase toward the seafloor, reaching a maximum of ~5 nmol/kg immediately above the seafloor in the North Pacific (Posacka et al., 2017; Zheng et al., 2021). The isotope ratios of Cu (δ^{65}Cu) are observed to be in the range of +0.4‰ to +0.8‰ in the surface water and +0.6‰ to +0.9‰ in the deep water (>1000 m) (Baconnais et al., 2019; Little, 2018; Takano, 2017; Takano et al., 2014; Thompson and Ellwood, 2014; Yang, 2020). These distributions are explained by the supply of isotopically light Cu from the continents to the surface water and scavenging of isotopically light Cu by particles (Takano et al., 2014). The mass balances of Ni, Cu, and Zn isotopes in the ocean have been evaluated, but they are currently unbalanced (Ciscato et al., 2018; Little et al., 2020; Little et al., 2014; Vance et al., 2016). This is due to the lack of information on riverine, atmospheric, and benthic inputs and sedimentary outputs. In this study, we investigate the concentrations and isotopic ratios of Ni, Cu, and Zn along the flow path from the North Equatorial Current to the Kuroshio through the East China Sea (ECS), and discuss the sources and behavior of Ni, Cu, and Zn by combining previously published data on Zn (Liao et al., 2020).

2. Methods

2.1. Sampling area

In this study, seawater samples were collected on the KH 15–3 cruise from one station in the continental shelf region, three stations in the Okinawa Trough, and one station slightly outside the ECS (Fig. 1). Seawater samples from the western North Pacific were collected at a KH 14–7 cruise station. The latitude and longitude of each station are shown in Supplementary Table 1.

The Kuroshio Current enters the ECS from the east coast of Taiwan and flows into the North Pacific Ocean through the Okinawa Trough. High-salinity water (34.6–35.0) above 200 m at AND06, AND22, AND31, and AND34 (Figs. 2 and 3) are mainly from the Kuroshio surface water (KSW). Low-salinity water above 50 m at AND26 indicates the inflow of the Changjiang diluted water (CDW) (Zhou et al., 2018). The salinity minimum at the depth of ~600 m at AND06, AND22, AND31, and AND34 originates from the North Pacific Intermediate Water, which flows into the ECS (Nakamura et al., 2013). The deep water (>1000 m) in the Okinawa Trough exhibits a salinity of 34.4–34.7, which originates from the deep water of the western North Pacific and enters through the Kerama Strait (Nakamura et al., 2013).

Large amounts of natural and anthropogenic materials flow into the ECS via the Changjiang River, which is the largest river in Asia (Guo and Yang, 2016; Yin et al., 2015), or via atmospheric aerosols present at high concentrations (Hsu et al., 2010; Park et al., 2019; Xie et al., 2016). Nakaguchi et al. (2020) determined the concentration of dissolved and labile-particulate trace metals (Al, Mn, Fe, Co, Ni, Cu, Zn, Cd, and Pb) in seawater samples collected during the same cruise as this study (KH

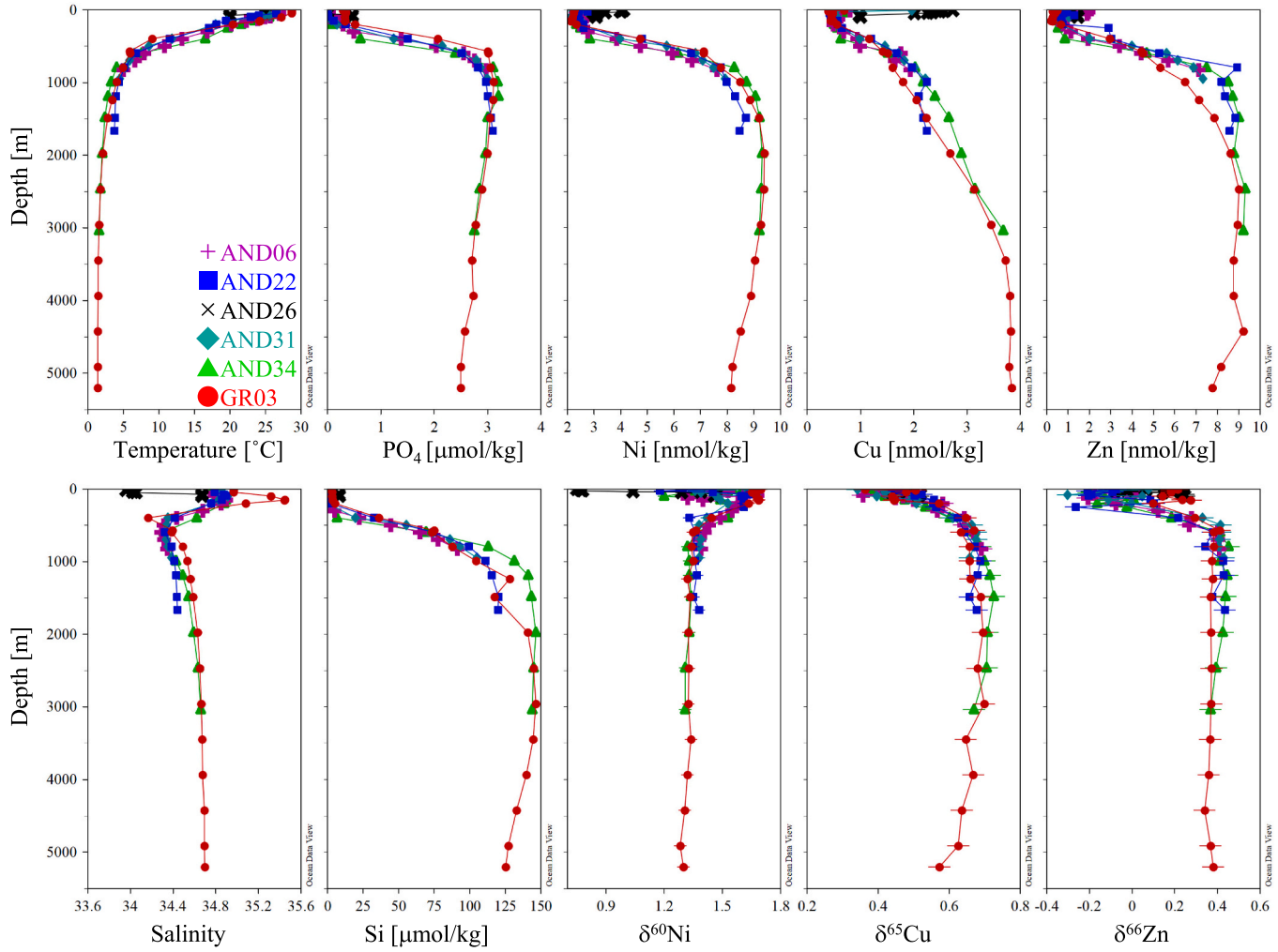

Fig. 2. Full depth profiles of temperature, salinity, concentrations of PO_4, Si, Ni, Cu, and Zn, and isotope ratios of Ni, Cu, and Zn. Data for Zn concentrations and δ^{66}Zn are from Liao et al. (2020), and temperature, salinity, and macronutrient concentrations are from Nakaguchi et al. (2020). Error bars for δ^{60}Ni, δ^{65}Cu, and δ^{66}Zn represent 2-standard deviations for replicate analyses of seawater samples (Takano et al., 2017).

15–3) and found high concentrations of these elements in the continental shelf region. They suggested that dissolved Fe and Al dominantly originated from lithogenic materials, but the other trace metals were additionally supplied by anthropogenic input and/or the reduction of manganese oxide in the shelf sediments. Liao et al. (2020) revealed the distribution of Zn isotope ratios in the ECS and western North Pacific by analyzing seawater samples collected on cruises including KH15–3. They observed isotopically light Zn in these regions and attributed the source of this light Zn to continental margin sediments or anthropogenic aerosols based on the box model approach and correlation between dissolved Zn concentrations and atmospheric optical depth. Liao and Ho (2018) determined the elemental compositions (Al, P, Ti, V, Mn, Fe, Co, Ni, Cu, Zn, Pb, Cd, and Mo) in suspended particles collected on the KH 15–3 and identified that the major source of Cd is biogenic particles, of Al, Ti, Mn, and Fe is lithogenic particles, and of Zn, Cu, Ni, Co, V, Mo, and Pb is anthropogenic aerosols. Signs of anthropogenic emissions can also be found in marine sediments of the East China Sea. These are rich in heavy metals, presumably due to anthropogenic emissions associated with agriculture, aquaculture, maritime transport, motor vehicle transport, and industrial waste (Zhang et al., 2020a).

2.2. Sampling

The sampling system for seawater is described in detail in Nakaguchi et al. (2020). Seawater samples were collected using Niskin-X bottles mounted on an epoxy-painted carousel. The carousel was hung on a Vectran or titanium-armored cable to settle it in the ocean. The inside of Niskin-X bottles was coated with Teflon and cleaned with 1% detergent and 0.1 mol/L hydrochloric acid (HCl). The collected seawater samples were filtered through a 0.2 μm AcroPak cartridge filter (Pall) and collected in Nalgene low-density polyethylene (LDPE) bottles (Thermo Fisher Scientific). The Nalgene LDPE bottles were pre-cleaned with 5% alkaline detergent (SCAT-20X; Nacalai Tesque), 3 mol/L HCl (reagent grade; Fujifilm Wako Chemicals), and 1 mol/L nitric acid (HNO_3, Ultrapur-100; Kanto Chemicals). Hydrochloric acid (Ultrapur-100; Kanto Chemicals) was added to the seawater samples to reach 0.02 mol/L. The seawater samples were stored in plastic containers for ~2.5 years (samples from KH 15–3) or ~7 years (samples from KH 14–7) before analysis.

2.3. Sample analysis

The perfluoroalkoxy alkane vials and LDPE bottles used for chemical separation were cleaned with 5% alkaline detergent and 4 mol/L HNO_3 (reagent grade; Fujifilm Wako Chemicals).

The isotope ratios of Ni, Cu, and Zn in seawater samples were determined using the method described by Takano et al. (2017) and Liao et al., (2020). Briefly, double spikes of ^{61}Ni—^{62}Ni and ^{67}Zn—^{70}Zn were

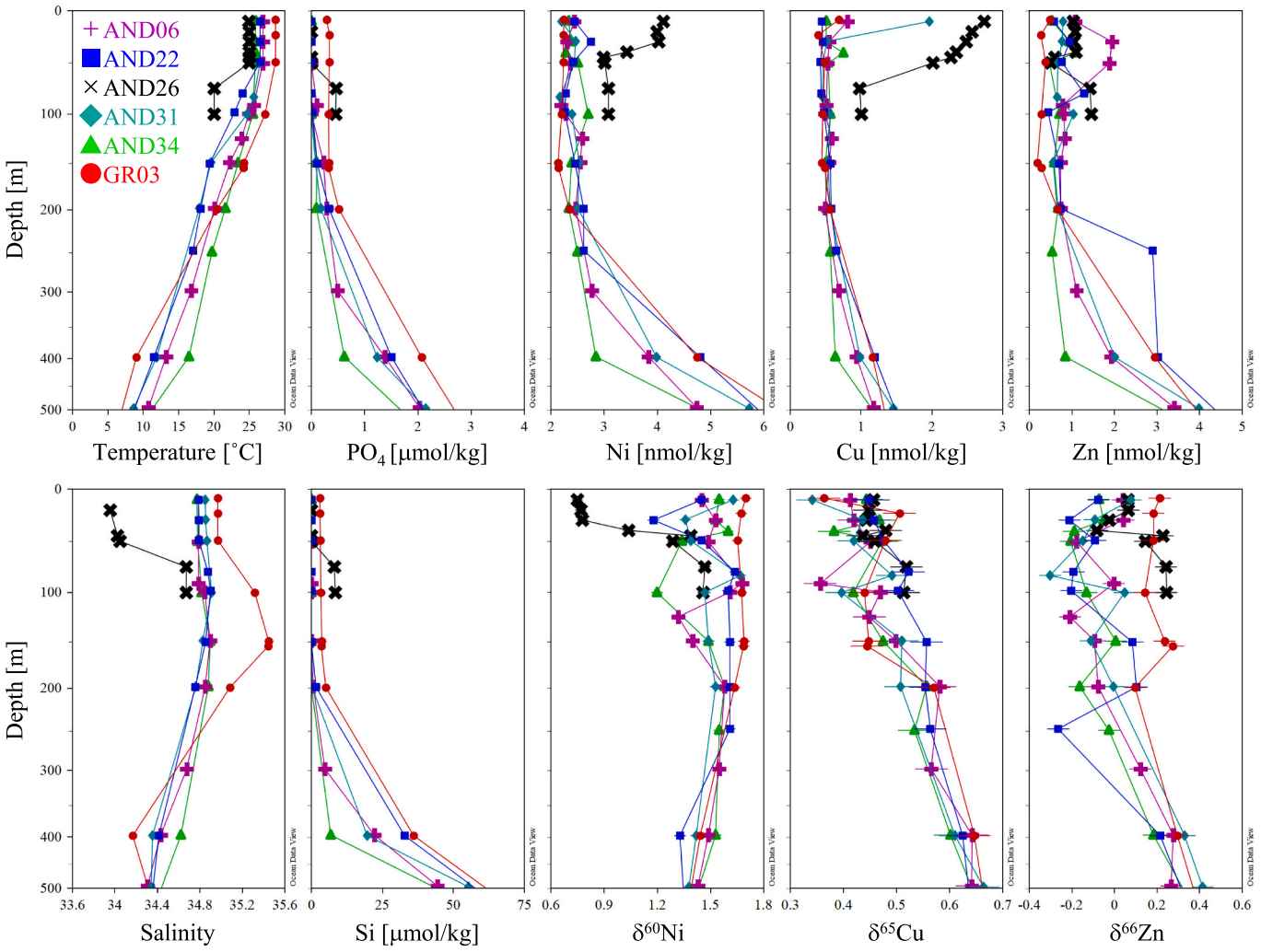

Fig. 3. Depth profiles of temperature, salinity, concentrations of PO_4, Si, Ni, Cu, and Zn, and isotope ratios of Ni, Cu, and Zn in water columns shallower than 500 m. Data for Zn concentrations and δ^{66}Zn are from Liao et al. (2020), and temperature, salinity, and macronutrient concentrations are from Nakaguchi et al. (2020). Error bars for δ^{60}Ni, δ^{65}Cu, and δ^{66}Zn represent 2-standard deviations for replicate analyses of seawater samples (Takano et al., 2017).

added to 1–2 L of the seawater sample and left overnight. The seawater sample was adjusted to pH 4.5–4.8 with an ammonium acetate buffer, and subsequently passed through a NOBIAS Chelate PA1W column (Hitachi High Technologies) to extract Ni, Cu, and Zn from seawater. The extracted Ni, Cu, and Zn were dissolved in 10 mol/L HCl (Kanto Chemicals) and loaded into a column packed with AG MP-1M anion exchange resin (Bio-Rad). Then, 10 mol/L HCl, 4 mol/L HCl, and 1 mol/L HNO_3 (Ultrapur-100; Kanto Chemicals) were used to elute Ni, Cu, and Zn, respectively, from the column. The eluates were evaporated, and the residues were dissolved in 1–2 mL of 0.3 mol/L HNO_3 after decomposition of organic matter with concentrated HNO_3 (Ultrapur-100, Kanto Chemicals) and hydrogen peroxide (H_2O_2, Tamapure-AA-100, Tama Chemicals).

Detailed conditions for measuring the concentrations and isotope ratios of Ni, Cu, and Zn are described by Liao et al. (2020) and Takano et al. (2021). The isotope ratios of Ni and Cu were measured using a NEPTUNE Plus MC-ICP-MS under a high-resolution mode for Ni, and Zn, and under a medium-resolution mode for Cu. Samples were introduced into the MC-ICP-MS using a PFA microflow nebulizer and an Aridus II desolvating system for Ni and Zn and using a PFA microflow nebulizer and a glass spray chamber for Cu. The isotopic fractionation of Ni and Zn during chemical separation and measurement was corrected using the double-spike method (Siebert et al., 2001). The isotopic fractionation of Cu during the measurements was corrected using an external correction method with Ga-doping. Concentrations were determined using the isotope dilution method for Ni and Zn, and the internal standard method with Ga-doping for Cu at the same time as the isotopic measurements.

The accuracy and precision of this method have been evaluated by Takano et al. (2017). The total procedure blanks were 0.004 nmol for Ni, 0.005 nmol for Cu, and 0.008 nmol for Zn, which were less than 0.09% for Ni, 1% for Cu, and 2% for Zn of the amounts of each element in the seawater sample. The external precision of isotopic analysis (2σ) for Ni, Cu, and Zn in seawater was ±0.03‰ for δ^{60}Ni, ±0.03‰ for δ^{65}Cu, and ±0.05‰ for δ^{66}Zn.

3. Results

Data for Ni and Cu at stations in the ECS and those for Ni, Cu, and Zn at a station in the western Pacific Ocean are shown in Supplementary Table S1. Data on Zn, macronutrients, and basic hydrographic parameters in the ECS have been reported in previous studies (Liao et al., 2020; Nakaguchi et al., 2020). Vertical profiles of the concentrations and isotope ratios of Ni, Cu, and Zn are shown in Fig. 2. and Fig. 3, together with the salinity, temperature, and macronutrient concentrations. The sectional distributions of the parameters in the ECS are shown in Fig. 4. Liao et al. (2020) showed very low δ^{66}Zn (−0.91‰) for a sample collected at 100 m of AND06. Recently, however, we found that the ^{62}Ni signal intensity detected in the isotopic measurement of Zn in this

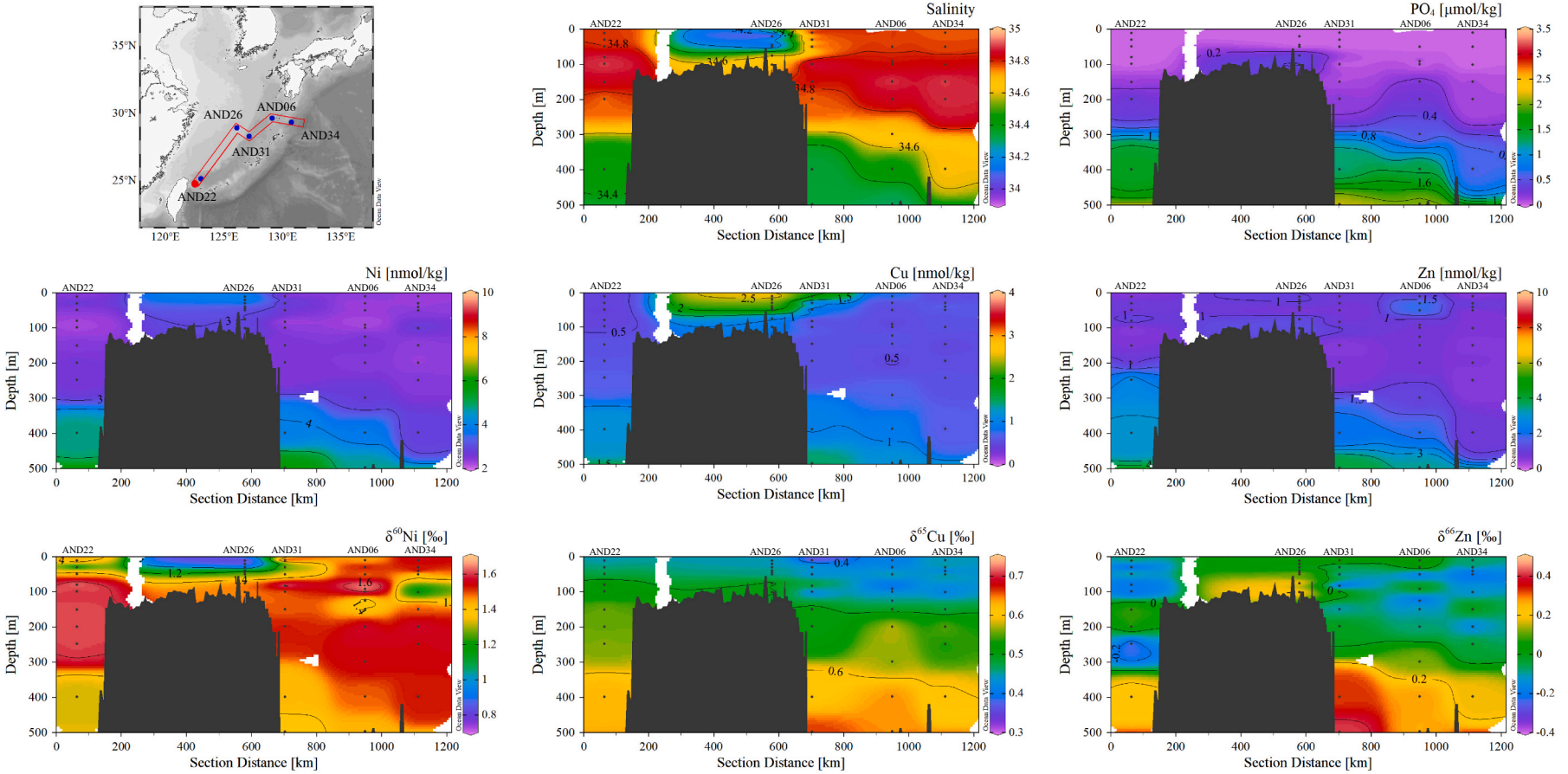

Fig. 4. Sectional distributions of salinity, concentrations of PO_4, Ni, Cu, and Zn, and isotope ratios of Ni, Cu, and Zn at depths shallower than 500 m in the East China Sea. The x-axis represents the distance from a red circle along a red line on the map. (For interpretation of the references to colour in this figure legend, the reader is referred to the web version of this article.)

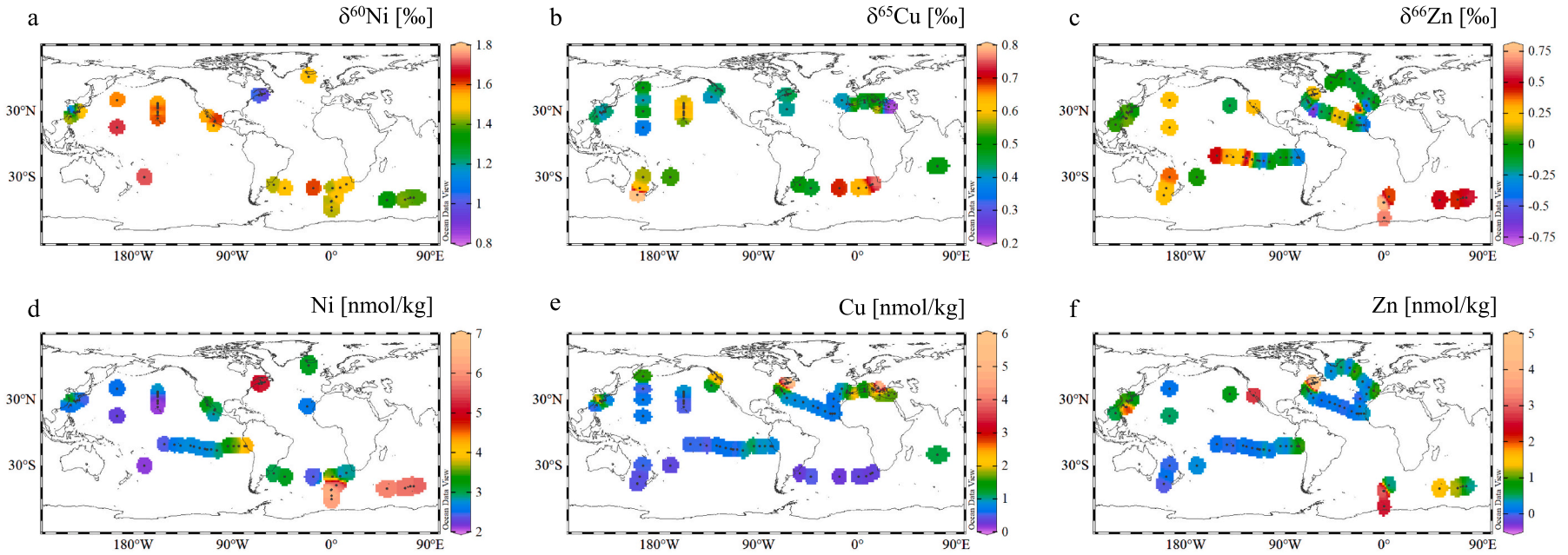

Fig. 5. Mapping of isotope ratios and concentrations of Ni (a, d), Cu (b, e), and Zn (c, f) in the uppermost surface sample at each station. Data on Ni are from Archer et al., 2020; Cameron and Vance, 2014; Schlitzer, 2018; Takano, 2017; Wang et al., 2019; Yang, 2020, 2021; on Cu from Baconnais et al., 2019; Little, 2018; Schlitzer, 2018; Takano, 2017; Takano et al., 2014; Thompson and Ellwood, 2014; Yang, 2020; and on Zn from Conway and John, 2014, 2015; John, 2007; John et al., 2018; Lemaitre, 2020; Liao, 2020; Samanta et al., 2017; Schlitzer, 2018; Vance et al., 2019; Wang et al., 2019; Zhao et al., 2014. The data off the coast of Canada are from the analysis of seawater reference materials (NASS-6 and CASS-5, National Research Council Canada), which is reported in Takano et al., 2017. Stations with no data available at depths shallower than 60 m are excluded.

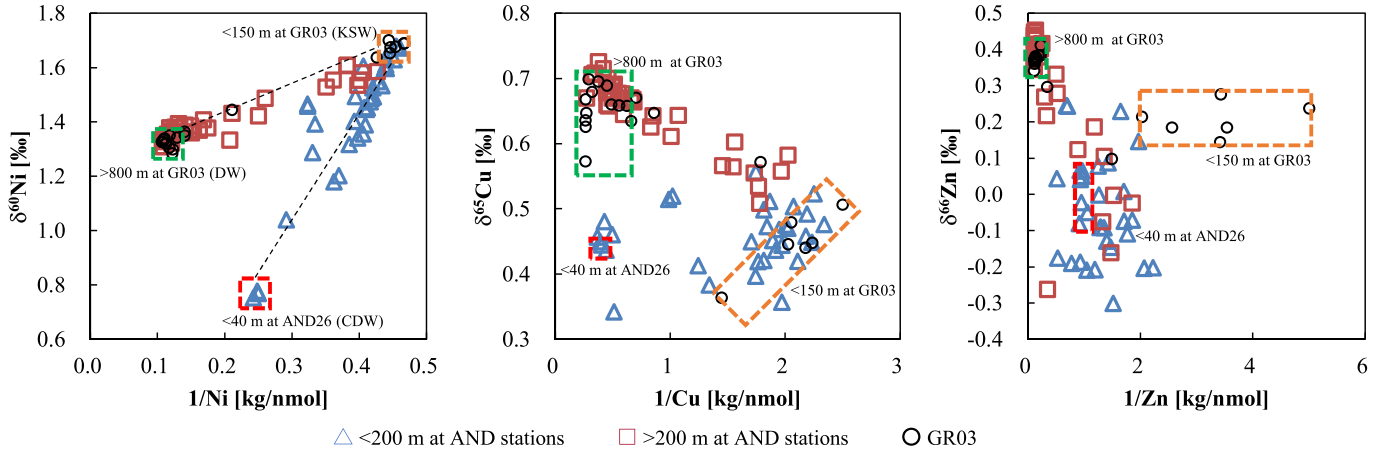

Fig. 6. Isotope ratios plotted against reciprocal concentrations for Ni, Cu, and Zn. Green and orange dotted squares represent the ranges of data for deep water (>800 m) and surface water (<150 m) at GR03, respectively. A red dotted square represents the range of data for surface water (<40 m) at AND26. (For interpretation of the references to colour in this figure legend, the reader is referred to the web version of this article.)

sample was higher (equivalent to 6% of the ^{64}Zn signal intensity) than that in the other samples (less than 1% of the ^{64}Zn signal intensity). In isotopic measurements of Zn, ^{64}Ni causes isobaric interference on ^{64}Zn. This interference is corrected by the signal intensity of ^{62}Ni and the natural abundance of Ni isotopes (Liao et al., 2020) but is not accurately corrected when the ^{62}Ni intensity is high. Therefore, we removed the δ^{66}Zn datum at 100 m depth of AND06.

From the same samples as the KH15–3 cruise, Nakaguchi et al. (2020) reported concentrations of Al, Mn, Fe, Co, Ni, Cu, Zn, Cd, and Pb; although their analytical method is different from that used in this study, our results regarding the concentrations of Ni, Cu, and Zn agree with theirs within a 20% error (Supplementary Fig. S1).

At depths deeper than 500 m, the concentrations of Ni, Cu, and Zn at stations in the ECS are similar to those at GR03 in the western North Pacific. Concentrations of Ni and Cu above 30 m at AND26 are significantly higher than those at other stations. Zinc concentrations at depths shallower than 150 m in the ECS are higher and more variable than those at GR03.

At depths deeper than 500 m, δ^{60}Ni is around +1.3‰, which is consistent with literature data in the deep waters of the global ocean (Archer et al., 2020; Cameron and Vance, 2014; Takano et al., 2017; Wang et al., 2019; Yang et al., 2020; Yang et al., 2021). At depths shallower than 500 m at GR03, δ^{60}Ni increases monotonically toward the surface, but some minima are observed at AND06, AND22, AND31, and AND34. At AND 26, and the lowest δ^{60}Ni (+0.75‰) is found at 11 m. At depths deeper than 500 m, δ^{65}Cu is in the range of +0.57 to +0.74‰ and becomes lower toward the surface. This profile is typical of the Pacific Ocean (Takano et al., 2014). δ^{66}Zn is in the ranges of +0.34 to +0.45‰ at depths deeper than 500 m and decreases at shallower depths. At depths shallower than 150 m, δ^{66}Zn is lower at stations in the ECS (−0.30‰ to +0.25‰) than at GR03 (+0.14‰ to +0.28‰).

4. Discussion

4.1. Sources of trace metals in the East China Sea

4.1.1. Nickel

In the open ocean, dissolved Ni concentrations are lower and δ^{60}Ni values are higher in surface water than those in deep water because phytoplankton preferentially takes up light Ni isotopes (Archer et al., 2020; Takano et al., 2017; Yang et al., 2021). However, δ^{60}Ni decreases in the surface water at stations in the ECS. In the surface water at AND26, where the CDW is the dominant water mass (Fig. 4), δ^{60}Ni is +0.75‰. In the CDW, high concentrations of Ni, Mn, Co, Cu, and Pb have been reported (Nakaguchi et al., 2020); thereby suggesting a supply of trace metals from the Changjiang River. Fig. 5a and d show global maps representing the Ni concentrations and δ-values of the shallowest samples at each station (Archer et al., 2020; Cameron and Vance, 2014; Schlitzer et al., 2018;Takano et al., 2017; Wang et al., 2019; Yang et al., 2020; Yang et al., 2021). Nickel concentrations are high and δ^{60}Ni values are low in the Southern Ocean owing to the intense vertical mixing of the water column. In the subtropical North Pacific, South Pacific, and Atlantic, isotope ratios of Ni become heavier with decreasing concentrations, probably owing to biological uptake. Compared with the distal ocean, our δ^{60}Ni values are evidently lower, corresponding to the increasing concentrations in the ECS and coastal waters off the east coast of Canada (Fig. 5), suggesting that δ^{60}Ni supplied from continental sources is substantially lower than that in seawater. Published data for δ^{60}Ni have a mean value of +0.80‰ for river water (Cameron and Vance, 2014), +0.33‰ for atmospheric aerosols (Takano et al., 2020), and +0.18‰ for rainwater (Takano et al., 2021). Ciscato et al. (2018) estimate that the δ value of total Ni supplied from rivers and the atmosphere to the ocean is +0.79‰. Therefore, it is reasonable that the low δ^{60}Ni observed in coastal regions is due to atmospheric and riverine inputs of Ni from the continent.

The lowest δ^{60}Ni in the ECS is +0.75‰, which is observed in the CDW. Assuming that this light Ni is supplied from the Changjiang River, δ^{60}Ni of the riverine input is expected to be less than +0.75‰. However, dissolved δ^{60}Ni in the middle reaches of this river is as high as ~1.3‰ (Cameron and Vance, 2014). One possible explanation for this discrepancy is the release of isotopically light Ni from sediments to the estuary of the Changjiang River. Fieldwork conducted in the Amazon basin has reported isotopic variations of Ni in river water resulting from the adsorption of isotopically light Ni on Fe oxyhydroxides (Revels et al., 2021). Furthermore, dissolved Ni is taken up by phytoplankton and partitioned into the particulate phase in estuarine blooms (Zhang et al., 2020b). Based on the distribution of δ^{60}Ni in the ocean, lighter isotopes are preferentially taken up by phytoplankton (Archer et al., 2020; Takano, 2017; Yang, 2021). Therefore, when Fe oxyhydroxides or biogenic particles accumulated in estuarine sediments are decomposed via diagenetic processes, isotopically light Ni may be released into the coastal ocean. Another possible explanation is the additional Ni input into the lower reaches and estuary. The lower reaches of the Changjiang River are highly industrialized and populous. Wen et al. (2013) found that dissolved Ni concentrations drastically increased in the lower reaches due to inputs from industries and municipal sewage in the Changjiang River. Associated with the increase in Ni concentrations owing to anthropogenic inputs, δ^{60}Ni may vary in the lower reaches. Anthropogenic activities likely emit the isotopically light Ni. Crude oil contains a large amount of Ni (291 ppm at the maximum; López and Lo

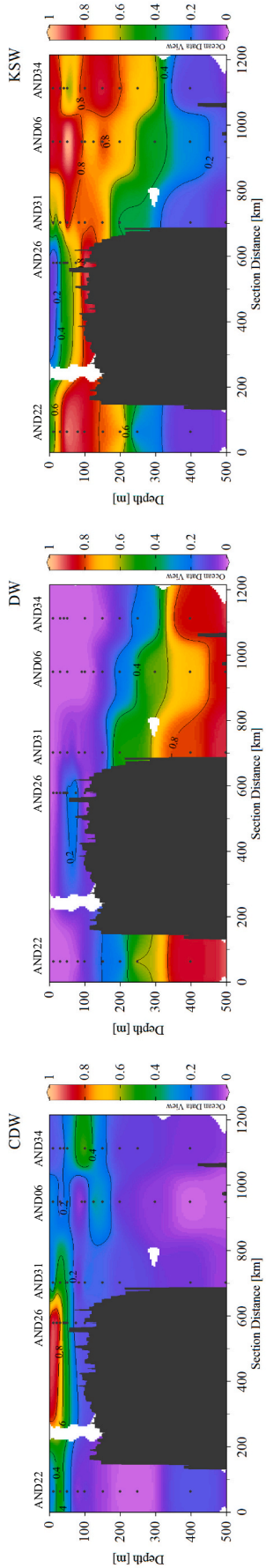

Fig. 7. Contributions of Ni supplied from Changjiang diluted water (CDW), deep water in the western North Pacific (DW), and Kuroshio surface water (KSW). This is estimated from concentrations and isotope ratios for Ni using the simple mixing model of three endmembers.

Mónaco, 2017), with δ^{60}Ni values ranging from +0.4 to +0.7‰(Ventura et al., 2015), and its combustion is the main source of Ni in the urban atmosphere (Peltier et al., 2008; Peltier and Lippmann, 2009; Wu et al., 2019). This atmospheric Ni may be supplied to rivers and coastal oceans through wet and dry deposition. Based on the rainwater samples collected in western Japan, the main source of dissolved Ni is determined to be crude oil combustion, and the δ^{60}Ni values range from −0.39 to +0.72‰ (Takano et al., 2021), which is lighter than the dissolved δ^{60}Ni in the middle reaches of the Changjiang River (Cameron and Vance, 2014).

4.1.2. Copper

In deep water (>600 m), δ^{65}Cu at the ECS stations is in the narrow range (0.69 ± 0.02‰, mean ± SD, n = 12) and indistinguishable from that at the western North Pacific stations, including GR03 (0.65 ± 0.05‰, n = 28, Takano et al., 2014), suggesting that Cu in the deep water of the ECS originates from the western North Pacific, as in the case of Ni (Fig. 2).

In surface water (<200 m), Cu concentrations increase to 2.8 nmol/kg, and δ^{65}Cu decreases to +0.4‰ in the ECS (Fig. 3). Globally, the Mediterranean Sea and the coastal waters of the western and eastern coasts of North America also have lower δ^{65}Cu and higher Cu concentrations than those in the central North Pacific and mid-Atlantic (Fig. 5b) (Baconnais et al., 2019; Little et al., 2018; Schlitzer et al., 2018;Takano et al., 2017; Takano et al., 2014; Thompson and Ellwood, 2014; Yang et al., 2020). This implies that the supply of isotopically light Cu occurs not only in the ECS but also in the coastal regions around the world and extends to the open ocean. Little et al. (2014) estimate the dissolved Cu fluxes from natural continental sources (mineral dust and rivers) to the global ocean and suggest that the Cu flux from rivers is the dominant source, with an average δ^{65}Cu of +0.68‰, which is higher than that of the coastal surface water. Therefore, undocumented sources of isotopically light Cu exist. Little et al. (2018) suggest the dissolution of particles in an estuary as the reason for the presence of isotopically light Cu in the surface water of the Argentine Basin. Particulate δ^{65}Cu ranges from −0.2 to +0.3‰ in the Amazon River system (Guinoiseau et al., 2018) and from −1.0 to −0.2‰ in the Itchen Estuary because the light isotopes of Cu preferentially partition to the particles in river water. Anthropogenic Cu is also a potential source of isotopically light Cu. Polluted atmospheric aerosols are enriched in Cu, with a mean δ^{65}Cu value of +0.2‰ in the South China Sea (Takano et al., 2020), +0.4‰ in São Paulo (Souto-Oliveira et al., 2018), and +0.3‰ in London (Dong et al., 2017). Rainwater in western Japan contains anthropogenic materials and has a mean δ^{65}Cu of +0.2‰ (Takano et al., 2021). The δ^{65}Cu varies from +0.2‰ to −0.7‰ downstream of the Garonne River, which is affected by anthropogenic activities (Petit et al., 2013).

The Cu concentrations at depths above 40 m are significantly higher at AND26 than those at other stations. This is likely owing to the input of Cu from the CDW. At depths shallower than 40 m at AND26, where the CDW dominates, δ^{65}Cu is ~0.5‰ and indistinguishable from that in the surface water at other stations. Dissolved δ^{65}Cu in the Changjiang River reaches a maximum of +1.5‰ in the middle reaches and gradually decreases downstream owing to the Cu input by weathering of ore deposits and/or industrial activities and ~0.6‰ at most of the stations in the lower reaches (Wang et al., 2020). The δ^{65}Cu in the lower reaches is consistent with that in the CDW observed in our study. However, we also note that high δ^{65}Cu +1.2‰ is observed at the most downstream site in the Changjiang River (Wang et al., 2020). This is considerably higher than the δ^{65}Cu in the CDW, suggesting that additional Cu input or isotopic fractionation may occur further downstream, including in the estuary.

4.1.3. Zinc

The Zn isotope ratios in the ECS have already been reported by Liao et al. (2020); it is discussed again here for reinterpretation with the updated Zn data in the global ocean and comprehensive knowledge in

comparison with Ni and Cu. At depths deeper than 800 m in the ECS, δ^{66}Zn is within a narrow range (+0.37 to +0.45‰) and similar to that in the deep water at GR03 (+0.34 to +0.38‰). At depths shallower than 200 m, δ^{66}Zn in the ECS and at GR03 is lower than that in deep water and lower in the ECS (−0.05‰ on average) than that at GR03 (+0.21‰). The δ^{66}Zn demonstrates a large range of variation (−0.8 to +0.8‰) in the surface water of the global ocean (Fig. 5f). Although the average δ^{66}Zn in surface water (−0.01‰) is lower than that in deep water (+0.38‰), high δ^{66}Zn is observed at some stations (e.g., the Southern Ocean and the central equatorial Pacific). There have been different explanations for this variation. The first is biological uptake of isotopically light Zn by phytoplankton and rapid remineralization of Zn in the subsurface water (Samanta et al., 2017; Vance et al., 2019). The second is scavenging of isotopically heavy Zn onto biogenic particles in conjunction with remineralization of intracellular light Zn (John and Conway, 2014; Weber et al., 2018). The third is the supply of anthropogenic light Zn to surface water from aeolian and riverine sources (Lemaitre et al., 2020; Liao et al., 2021; Liao et al., 2020). Fig. 5 illustrates that the δ^{66}Zn is low in the coastal waters off the west coast of Africa, the west coast of South America, and the east coast of North America, the Philippine Sea, and the South China Sea, as well as in the ECS, which seems to supply isotopically light Zn from the continents.

The increase in Zn concentration in the CDW is less apparent than that of Ni (Fig. 4), although the dissolved Zn flux is ~4 times higher than that of dissolved Ni in the lower reaches of the Changjiang River (Wen et al., 2013). This unclear signature of Zn supply from the CDW may be because Zn is readily taken up by phytoplankton or adsorbed onto biologenic particles. In fact, Zn is more abundant in phytoplankton than Ni and Cu (Twining and Baines, 2013).

The δ^{66}Zn values in the surface water (<200 m) at AND06, AND22, AND31, and AND34 are lower than those in the surface water (<40 m) at AND26, where the CDW is located (Fig. 4). It seems that δ^{66}Zn (−0.2 to +0.0‰) is low in the surface water of the ECS and slightly higher δ^{66}Zn (+0.0 to +0.2‰) is spread from the CDW. Zinc is highly enriched in anthropogenic aerosols, which are mostly soluble in water (Jiang et al., 2014). Generally, anthropogenic aerosols have low δ^{66}Zn; −1.4 to +0.2‰ in Sao Paulo (Souto-Oliveira et al., 2018), −0.3 to +0.4‰ in London (Dong et al., 2017; Ochoa-Gonzalez et al., 2016), −0.8 to −0.6‰ in Barcelona (Ochoa-Gonzalez et al., 2016), and +0.0 to +0.4‰ in the northern South China Sea (Liao et al., 2021). Therefore, as suggested by Liao et al. (2020, 2021), anthropogenic Zn input via atmospheric aerosols may be responsible for the low δ^{66}Zn in the ECS, which is strongly influenced by anthropogenic aerosols from East Asia (Hsu et al., 2010). Slightly higher δ^{66}Zn values with higher Zn concentrations in the CDW may reflect the high δ^{66}Zn in the Changjiang River (+0.37‰ to +0.87‰, Little et al., 2014).

4.2. Mixing of dissolved metals in the East China Sea

To understand the mixing of dissolved metals in the ECS, δ-values are plotted against reciprocal concentrations for Ni, Cu, and Zn (Fig. 6). For Ni, two endmembers are found in the data from the western North Pacific station, GR03. One is the samples deeper than 800 m at GR03, which are plotted at +1.3‰ of δ^{60}Ni and 0.1 $(\text{nmol/kg})^{-1}$ of 1/Ni. Another is the samples at depths shallower than 200 m, which are plotted at +1.7‰ of δ^{60}Ni and 0.45 $(\text{nmol/kg})^{-1}$ of 1/Ni. The samples at depths of 200–800 m at GR03 are plotted along the mixing line between these two endmembers. The CDW (located at <40 m depths at AND26) is the third endmember with +0.7‰ of δ^{60}Ni and 0.25 $(\text{nmol/kg})^{-1}$ of 1/Ni. All samples at depths deeper than 200 m in the ECS are plotted along the mixing line of the deep/surface water at GR03. This is because the intermediate and deep waters in the western North Pacific flow into the ECS. Samples shallower than 200 m in the ECS are plotted along the mixing line of the CDW/GR03 surface water or between the two mixing lines, which reflects mixing of KSW derived from the surface water in the western North Pacific, deep water (DW) entering from the western North Pacific, and the CDW derived from the Changjiang River. The low concentration and heavy isotope ratio for Ni in the KSW are caused by biological uptake of isotopically light Ni. The high concentration and light isotope ratio for Ni in the CDW is owing to the input from the continents.

Clearly distinguishable endmembers enable the source apportionment of Ni. Assuming simple mixing of Ni in the CDW, KSW, and DW, their mixing proportions are calculated based on Eqs. (1) and (2).

$$C_{SMP} = C_{CDW}F_{CDW} + C_{DW}F_{DW} + C_{KSW}F_{KSW} \quad (1)$$

$$C_{SMP}\delta_{SMP} = C_{CDW}F_{CDW}\delta_{CDW} + C_{DW}F_{DW}\delta_{DW} + C_{KSW}F_{KSW}\delta_{KSW} \quad (2)$$

$$F_{CDW} + F_{DW} + F_{KSW} = 1 \quad (3)$$

where F denotes the mixing proportions of endmembers. C is the Ni concentration in the endmembers and the individual sample (SMP), and δ is δ^{60}Ni in the endmembers and the individual sample. C_{CDW} and δ_{CDW} are 4.1 nmol/kg and +0.77‰, respectively, which are the means of their values in samples of 0–40 m at AND26. C_{DW} and δ_{DW} are 8.5 nmol/kg and +1.35‰, respectively, which are their values in samples at 1000 m depth of GR03. C_{KSW} and δ_{KSW} are 2.2 nmol/kg and +1.68‰, respectively, which are the means of their values in samples shallower than 150 m at GR03. Mixing proportions of the endmembers are calculated by Eqs. (4)–(6) derived from Eqs. (1)–(3). The contributions of Ni supplied by each endmember to the total Ni concentration are calculated using Eq. (7).

$$F_{CDW} = \frac{C_{SMP}(C_{KSW}(\delta_{SMP} - \delta_{KSW}) + C_{DW}(\delta_{DW} - \delta_{SMP})) + C_{DW}C_{KSW}(\delta_{KSW} - \delta_{DW})}{C_{KSW}(C_{DW}(\delta_{KSW} - \delta_{DW}) + C_{CDW}(\delta_{CDW} - \delta_{KSW})) + C_{CDW}C_{DW}(\delta_{DW} - \delta_{CDW})} \quad (4)$$

$$F_{DW} = \frac{C_{SMP}(C_{KSW}(\delta_{KSW} - \delta_{SMP}) + C_{CDW}(\delta_{SMP} - \delta_{CDW})) + C_{CDW}C_{KSW}(\delta_{CDW} - \delta_{KSW})}{C_{KSW}(C_{DW}(\delta_{KSW} - \delta_{DW}) + C_{CDW}(\delta_{CDW} - \delta_{KSW})) + C_{CDW}C_{DW}(\delta_{DW} - \delta_{CDW})} \quad (5)$$

$$F_{KSW} = \frac{C_{SMP}(C_{DW}(\delta_{SMP} - \delta_{DW}) + C_{CDW}(\delta_{CDW} - \delta_{SMP})) + C_{CDW}C_{DW}(\delta_{DW} - \delta_{CDW})}{C_{KSW}(C_{DW}(\delta_{KSW} - \delta_{DW}) + C_{CDW}(\delta_{CDW} - \delta_{KSW})) + C_{CDW}C_{DW}(\delta_{DW} - \delta_{CDW})} \quad (6)$$

$$Contribution_X = \frac{C_X F_X}{C_{SMP}} \ (X = CDW, DW, \text{or } KSW) \quad (7)$$

Fig. 7 shows the estimated Ni contributions from the CDW, DW, and KSW in the ECS. Above 300 m at AND06, AND22, AND31, and AND34 in the Okinawa Trough, Ni originates from the KSW. Nickel in the CDW extends from AND26 to the subsurface water at the stations along the Kuroshio, with a maximum of 39% at AND31 (30 m) and 58% at AND22 (30 m). The contribution of Ni from DW increases with depth, reaching >50% at 500 m in the Okinawa Trough.

Unlike the case of Ni, the concentrations and isotopic ratios of Cu and Zn in the ECS cannot be explained by simple mixing (Fig. 6). This can be attributed to the complex biogeochemical processes in the ocean. The distribution of concentrations and isotope ratios may be dominated by biochemical processes, such as scavenging, biological uptake, and remineralization, rather than simple mixing. As discussed in Section 4.1.3, the concentrations and isotopic ratios of Zn from CDW may be modified by biological uptake. Moreover, Cu in the ocean is affected by stronger scavenging than Ni (Boyle et al., 1977; Takano et al., 2014; Zheng et al., 2021).

In addition, inputs from diverse sources with different elemental and isotopic compositions increase the number of endmembers and make the mixing line unclear. For example, if metals are supplied to the ECS by atmospheric deposition via a pathway independent of CDW, it becomes a new end member. Zinc likely has an additional endmember because anthropogenic Zn is observed in various environments, including rivers and the atmosphere (Araújo et al., 2021; Chen et al., 2008; Dong, 2017; Souto-Oliveira et al., 2018). Furthermore, reduction of Mn oxides releases adsorbed trace metals, which is a potential source of trace metals. Nakaguchi et al. (2020) suggest that Mn reduction in shelf sediments is one of the sources of trace metals in the ECS.

5. Conclusions

We revealed the distributions of dissolved Ni, Cu, and Zn and their isotope ratios in the ECS. The concentrations and isotope ratios of Ni, Cu, and Zn in deep water of the ECS are almost the same as those in the western North Pacific, which reflects the inflow of deep water from the western North Pacific. In the CDW, the concentrations of Ni, Cu, and Zn are 3.0–4.1 nmol/kg, 2.0–2.7 nmol/kg, and 0.5–1.1 nmol/kg, respectively. These concentrations are higher than those in the North Pacific, suggesting the supply of these elements from the continent. In the CDW, δ^{60}Ni ranges from +0.8 to +1.4‰, which is evidently lower than that in surface water of the Okinawa Trough and the western North Pacific (1.7‰). The distributions of concentrations and isotope ratios for Ni in the ECS are explained by simple mixing among the three endmembers (CDW, KSW, and DW in the western North Pacific). A mixing model using Ni isotope ratios and concentrations quantitatively evaluates the sources of dissolved Ni in the ECS. Dissolved Ni in the CDW extends to subsurface water at the stations along the Kuroshio (AND31 and AND06), with a maximum of 58% at 30 m depth. In the CDW, δ^{65}Cu ranges from +0.4 to +0.5‰ and δ^{66}Zn ranges from −0.1 to +0.2‰, which are close to those in the surface water of the Okinawa Trough but lower than those in the surface water of the distal ocean, such as the central Pacific. Compared with published data from the global ocean, dissolved Ni, Cu, and Zn are isotopically lighter in the surface water of some coastal regions than in the pelagic regions, indicating that isotopically light Ni, Cu, and Zn are supplied from the continents.

Declaration of Competing Interest

None.

Acknowledgement

We would like to thank the captain and crew of the KH 15-3 and KH 14-7 cruises for their help in collecting seawater samples. We are grateful to Katsuhiko Suzuki and Yusuke Fukami (Japan Agency for Marine-Earth Science and Technology) for the use of MC-ICPMS. This work was supported by the Joint Research Grant for Environmental Isotope Study from the Research Institute for Humanity and Nature, KAKENHI Grants (18K14250, 15H01727, 19H01148) from the Japan Society for the Promotion of Science, and the Future Development Funding Program of Kyoto University Research Coordination Alliance, Japan.

Appendix A. Supplementary data

Supplementary data to this article can be found online at https://doi.org/10.1016/j.marchem.2022.104135.

References

Araújo, D.F., Ponzevera, E., Weiss, D.J., Knoery, J., Briant, N., Yepez, S., Bruzac, S., Sireau, T., Brach-Papa, C., 2021. Application of Zn Isotope Compositions in Oysters to Monitor and Quantify Anthropogenic Zn Bioaccumulation in Marine Environments over Four Decades: A "Mussel Watch Program" Upgrade. ACS ES&T Water 1 (4), 1035–1046.

Archer, C., Vance, D., Milne, A., Lohan, M.C., 2020. The oceanic biogeochemistry of nickel and its isotopes: new data from the South Atlantic and the Southern Ocean biogeochemical divide. Earth Planet. Sci. Lett. 535, 116118.

Baconnais, I., Rouxel, O., Dulaquais, G., Boye, M., 2019. Determination of the copper isotope composition of seawater revisited: a case study from the Mediterranean Sea. Chem. Geol. 511, 465–480.

Boye, M., et al., 2012. Distributions of dissolved trace metals (Cd, Cu, Mn, Pb, Ag) in the southeastern Atlantic and the Southern Ocean. Biogeosciences 9 (8), 3231–3246.

Boyle, E.A., Sclater, F.R., Edmond, J.M., 1977. The distribution of dissolved copper in the Pacific. Earth Planet. Sci. Lett. 37 (1), 38–54.

Brand, L.E., Sunda, W.G., Guillard, R.R.L., 1986. Reduction of marine phytoplankton reproduction rates by copper and cadmium. J. Exp. Mar. Biol. Ecol. 96 (3), 225–250.

Cameron, V., Vance, D., 2014. Heavy nickel isotope compositions in rivers and the oceans. Geochim. Cosmochim. Acta 128 (0), 195–211.

Chen, J., Gaillardet, J., Louvat, P., 2008. Zinc Isotopes in the Seine River Waters, France: A Probe of Anthropogenic Contamination. Environ. Sci. Technol. 42 (17), 6494–6501.

Ciscato, E.R., Bontognali, T.R.R., Vance, D., 2018. Nickel and its isotopes in organic-rich sediments: implications for oceanic budgets and a potential record of ancient seawater. Geosciences 494, 239–250.

Conway, T.M., John, S.G., 2014. The biogeochemical cycling of zinc and zinc isotopes in the North Atlantic Ocean. Glob. Biogeochem. Cycles 28 (10), 1111–1128.

Conway, T.M., John, S.G., 2015. The cycling of iron, zinc and cadmium in the North East Pacific Ocean – insights from stable isotopes. Geochim. Cosmochim. Acta 164, 262–283.

Croot, P.L., Baars, O., Streu, P., 2011. The distribution of dissolved zinc in the Atlantic sector of the Southern Ocean. Deep-Sea Res. II Top. Stud. Oceanogr. 58 (25), 2707–2719.

Dong, S., et al., 2017. Isotopic signatures suggest important contributions from recycled gasoline, road dust and non-exhaust traffic sources for copper, zinc and lead in PM10 in London, United Kingdom. Atmos. Environ. 165, 88–98.

Guinoiseau, D., et al., 2018. Fate of particulate copper and zinc isotopes at the Solimões-Negro river confluence, Amazon Basin, Brazil. Chem. Geol. 489, 1–15.

Guo, Y., Yang, S., 2016. Heavy metal enrichments in the Changjiang (Yangtze River) catchment and on the inner shelf of the East China Sea over the last 150years. Sci. Total Environ. 543, 105–115.

Hsu, S.C., et al., 2010. Sources, solubility, and dry deposition of aerosol trace elements over the East China Sea. Mar. Chem. 120 (1–4), 116–127.

Jiang, S.Y.N., Yang, F., Chan, K.L., Ning, Z., 2014. Water solubility of metals in coarse PM and PM2.5 in typical urban environment in Hong Kong. Atmospheric. Pollut. Res. 5 (2), 236–244.

John, S.G., 2007. The marine biogeochemistry of zinc isotopes. WHOI Theses.
John, S.G., Conway, T.M., 2014. A role for scavenging in the marine biogeochemical cycling of zinc and zinc isotopes. Earth Planet. Sci. Lett. 394, 159–167.
John, S.G., Helgoe, J., Townsend, E., 2018. Biogeochemical cycling of Zn and Cd and their stable isotopes in the Eastern Tropical South Pacific. Mar. Chem. 201, 256–262.
Köbberich, M., Vance, D., 2019. Zn isotope fractionation during uptake into marine phytoplankton: implications for oceanic zinc isotopes. Chem. Geol. 523, 154–161.
Lemaitre, N., et al., 2020. Pervasive sources of isotopically light zinc in the North Atlantic Ocean. Earth Planet. Sci. Lett. 539, 116216.
Liao, W.-H., Ho, T.-Y., 2018. Particulate trace metal composition and sources in the Kuroshio adjacent to the East China Sea: the importance of aerosol deposition. J. Geophys. Res. Oceans 123 (9), 6207–6223.
Liao, W.-H., et al., 2020. Zn isotope composition in the water column of the northwestern Pacific Ocean: the importance of external sources. Glob. Biogeochem. Cycles 34 (1) e2019GB006379.
Liao, W.-H., et al., 2021. Zn elemental and isotopic features in sinking particles of the South China Sea: implications for its sources and sinks. Geochim. Cosmochim. Acta 314, 68–84.
Little, S.H., Vance, D., Walker-Brown, C., Landing, W.M., 2014. The oceanic mass balance of copper and zinc isotopes, investigated by analysis of their inputs, and outputs to ferromanganese oxide sediments. Geochim. Cosmochim. Acta 125 (0), 673–693.
Little, S.H., et al., 2018. Paired dissolved and particulate phase Cu isotope distributions in the South Atlantic. Chem. Geol. 502, 29–43.
Little, S.H., et al., 2020. Towards balancing the oceanic Ni budget. Earth Planet. Sci. Lett. 547, 116461.
López, L., Lo Mónaco, S., 2017. Vanadium, nickel and sulfur in crude oils and source rocks and their relationship with biomarkers: implications for the origin of crude oils in Venezuelan basins. Org. Geochem. 104, 53–68.
Middag, R., de Baar, H.J.W., Bruland, K.W., 2019. The relationships between dissolved zinc and major nutrients phosphate and silicate along the GEOTRACES GA02 transect in the West Atlantic Ocean. Glob. Biogeochem. Cycles 33 (1), 63–84.
Middag, R., de Baar, H.J.W., Bruland, K.W., van Heuven, S.M.A.C., 2020. The distribution of nickel in the West-Atlantic Ocean, its relationship with phosphate and a comparison to cadmium and zinc. Front. Mar. Sci. 7 (105).
Morel, F.M.M., Price, N.M., 2003. The biogeochemical cycles of trace metals in the oceans. Science 300 (5621), 944–947.
Nakaguchi, Y., et al., 2020. Distribution and stoichiometry of Al, Mn, Fe, Co, Ni, Cu, Zn, Cd, and Pb in the East China Sea. J. Oceanogr. 77, 463–485.
Nakamura, H., et al., 2013. Intermediate and deep water formation in the Okinawa trough. J. Geophys. Res. Oceans 118 (12), 6881–6893.
Ochoa-Gonzalez, R., et al., 2016. New insights from zinc and copper isotopic compositions into the sources of atmospheric particulate matter from two major European cities. Environ. Sci. Technol. 50 (18), 9816–9824.
Park, S., et al., 2019. Variability of aerosol optical properties observed at a polluted marine (Gosan, Korea) and a High-Altitude Mountain (Lulin, Taiwan) site in the Asian continental outflow. Aerosol Air Qual. Res. 19 (6), 1272–1283.
Peltier, R.E., Lippmann, M., 2009. Residual oil combustion: 2. Distributions of airborne nickel and vanadium within New York City. J. Expos. Sci. Environ. Epidemiol. 20, 342.
Peltier, R.E., Hsu, S.-I., Lall, R., Lippmann, M., 2008. Residual oil combustion: a major source of airborne nickel in New York City. J. Expos. Sci. Environ. Epidemiol. 19, 603.
Petit, J.C.J., et al., 2013. Anthropogenic sources and biogeochemical reactivity of particulate and dissolved Cu isotopes in the turbidity gradient of the Garonne River (France). Chem. Geol. 359 (0), 125–135.
Posacka, A.M., et al., 2017. Dissolved copper (dCu) biogeochemical cycling in the subarctic Northeast Pacific and a call for improving methodologies. Mar. Chem. 196, 47–61.
Revels, B.N., Rickli, J., Moura, C.A.V., Vance, D., 2021. Nickel and its isotopes in the Amazon Basin: the impact of the weathering regime and delivery to the oceans. Geochim. Cosmochim. Acta 293, 344–364.
Roshan, S., Wu, J., 2015. The distribution of dissolved copper in the tropical-subtropical North Atlantic across the GEOTRACES GA03 transect. Mar. Chem. 176, 189–198.
Ruacho, A., et al., 2020. Organic dissolved copper speciation across the U.S. GEOTRACES equatorial Pacific zonal transect GP16. Mar. Chem. 225, 103841.
Samanta, M., Ellwood, M.J., Sinoir, M., Hassler, C.S., 2017. Dissolved zinc isotope cycling in the Tasman Sea, SW Pacific Ocean. Mar. Chem. 192, 1–12.
Schlitzer, R., et al., 2018. The GEOTRACES intermediate data product 2017. Chem. Geol. 493, 210–223.
Siebert, C., Nägler, T.F., Kramers, J.D., 2001. Determination of molybdenum isotope fractionation by double-spike multicollector inductively coupled plasma mass spectrometry. Geochem. Geophys. Geosyst. 2 (7).
Souto-Oliveira, C.E., Babinski, M., Araújo, D.F., Andrade, M.F., 2018. Multi-isotopic fingerprints (Pb, Zn, Cu) applied for urban aerosol source apportionment and discrimination. Sci. Total Environ. 626, 1350–1366.
Takano, S., Tanimizu, M., Hirata, T., Sohrin, Y., 2014. Isotopic constraints on biogeochemical cycling of copper in the ocean. Nat. Commun. 5.
Takano, S., et al., 2017. A simple and rapid method for isotopic analysis of nickel, copper, and zinc in seawater using chelating extraction and anion exchange. Anal. Chim. Acta 967, 1–11.
Takano, S., et al., 2020. Sources of particulate Ni and Cu in the water column of the northern South China Sea: evidence from elemental and isotope ratios in aerosols and sinking particles. Mar. Chem. 219, 103751.
Takano, S., et al., 2021. Isotopic analysis of nickel, copper, and zinc in various freshwater samples for source identification. Geochem. J. 55 (3), 171–183.
Thompson, C.M., Ellwood, M.J., 2014. Dissolved copper isotope biogeochemistry in the Tasman Sea, SW Pacific Ocean. Mar. Chem. 165 (0), 1–9.
Twining, B.S., Baines, S.B., 2013. The trace metal composition of marine phytoplankton. Annu. Rev. Mar. Sci. 5 (1), 191–215.
Vance, D., et al., 2016. The oceanic budgets of nickel and zinc isotopes: the importance of sulfidic environments as illustrated by the Black Sea. Philos. Trans. R. Soc. A Math. Phys. Eng. Sci. 374 (2081).
Vance, D., de Souza, G.F., Zhao, Y., Cullen, J.T., Lohan, M.C., 2019. The relationship between zinc, its isotopes, and the major nutrients in the North-East Pacific. Earth Planet. Sci. Lett. 525, 115748.
Ventura, G.T., et al., 2015. The stable isotope composition of vanadium, nickel, and molybdenum in crude oils. Appl. Geochem. 59, 104–117.
Vu, H.T.D., Sohrin, Y., 2013. Diverse stoichiometry of dissolved trace metals in the Indian Ocean. Sci. Rep. 3.
Wang, R.M., Archer, C., Bowie, A.R., Vance, D., 2019. Zinc and nickel isotopes in seawater from the Indian Sector of the Southern Ocean: the impact of natural iron fertilization versus Southern Ocean hydrography and biogeochemistry. Chem. Geol. 511, 452–464.
Wang, Q., et al., 2020. The geochemical behavior of Cu and its isotopes in the Yangtze River. Sci. Total Environ. 728, 138428.
Weber, T., John, S., Tagliabue, A., DeVries, T., 2018. Biological uptake and reversible scavenging of zinc in the global ocean. Science 361 (6397), 72–76.
Wen, Y., Yang, Z., Xia, X., 2013. Dissolved and particulate zinc and nickel in the Yangtze River (China): distribution, sources and fluxes. Appl. Geochem. 31, 199–208.
Wu, S.-P., et al., 2019. Source apportionment of PM2.5 at urban and suburban sites in a Port City of Southeastern China. Aerosol Air Qual. Res. 19 (9), 2017–2031.
Xie, X., Liu, X., Wang, H., Wang, Z., 2016. Effects of aerosols on radiative forcing and climate over East Asia with different SO2 emissions. Atmosphere 7 (8), 99.
Yang, S.-C., et al., 2020. A new purification method for Ni and Cu stable isotopes in seawater provides evidence for widespread Ni isotope fractionation by phytoplankton in the North Pacific. Chem. Geol. 547, 119662.
Yang, S.-C., et al., 2021. Lack of redox cycling for nickel in the water column of the Eastern tropical north pacific oxygen deficient zone: insight from dissolved and particulate nickel isotopes. Geochim. Cosmochim. Acta 309, 235–250.
Yin, S., Feng, C., Li, Y., Yin, L., Shen, Z., 2015. Heavy metal pollution in the surface water of the Yangtze estuary: a 5-year follow-up study. Chemosphere 138, 718–725.
Zhang, M., Sun, X., Xu, J., 2020a. Heavy metal pollution in the East China Sea: a review. Mar. Pollut. Bull. 159, 111473.
Zhang, Z., et al., 2020b. Spatial variations of phytoplankton biomass controlled by river plume dynamics over the lower Changjiang estuary and adjacent shelf based on high-resolution observations. Front. Mar. Sci. 7 (906).
Zhao, Y., Vance, D., Abouchami, W., de Baar, H.J.W., 2014. Biogeochemical cycling of zinc and its isotopes in the Southern Ocean. Geochim. Cosmochim. Acta 125 (0), 653–672.
Zheng, L., Minami, T., Takano, S., Ho, T.-Y., Sohrin, Y., 2021. Sectional distribution patterns of Cd, Ni, Zn, and Cu in the North Pacific Ocean: relationships to nutrients and importance of scavenging. Glob. Biogeochem. Cycles 35 (7) e2020GB006558.
Zhou, P., et al., 2018. Water mass analysis of the East China Sea and interannual variation of Kuroshio subsurface water intrusion through an optimum multiparameter method. J. Geophys. Res. Oceans 123 (5), 3723–3738.